⌘ *Author's Choice*

THE JOURNAL OF BIOLOGICAL CHEMISTRY VOL. 286, NO. 19, pp. 17168–17180, May 13, 2011

The X Protein of Hepatitis B Virus Inhibits Apoptosis in Hepatoma Cells through Enhancing the Methionine Adenosyltransferase 2A Gene Expression and Reducing *S*-Adenosylmethionine Production*

Received for publication, July 23, 2010, and in revised form, January 16, 2011 Published, JBC Papers in Press, January 19, 2011, DOI 10.1074/jbc.M110.167783

Quanyan Liu[‡], Jiwei Chen[‡], Li Liu[‡], Jun Zhang[‡], Dongfeng Wang[‡], Lu Ma[§], Yueming He[‡], Yingle Liu[¶], Zhisu Liu[‡1], and Jianguo Wu[¶2]

From the [‡]Department of General Surgery, Research Center of Digestive Diseases, Zhongnan Hospital, [¶]State Key Laboratory of Virology, College of Life Sciences, and Chinese-French Liver Disease Research Institute at Zhongnan Hospital, Wuhan University, Wuhan 430071 and the [§]Department of Epidemiology and Hygienic Statistics, School of Public Health, Wuhan University, Wuhan 430072, China

The X protein (HBx) of hepatitis B virus (HBV) is involved in the development of hepatocellular carcinoma (HCC), and methionine adenosyltransferase 2A (*MAT2A*) promotes the growth of liver cancer cells through altering *S*-adenosylmethionine homeostasis. Thus, we speculated that a link between *HBx* and *MAT2A* may contribute to HCC development. In this study, the effects of *HBx* on *MAT2A* expression and cell apoptosis were investigated, and the molecular mechanism by which *HBx* and *MAT2A* regulate tumorigenesis was evaluated. Results from immunohistochemistry analyses of 37 pairs of HBV-associated liver cancer tissues/corresponding peritumor tissues showed that *HBx* and *MAT2A* are highly expressed in most liver tumor tissues. Our *in vitro* results revealed that *HBx* activates *MAT2A* expression in a dose-dependent manner in hepatoma cells, and such regulation requires the *cis*-regulatory elements *NF-κB* and *CREB* on the *MAT2A* gene promoter. Electrophoretic mobility shift assay (EMSA) and chromatin immunoprecipitation (ChIP) further demonstrated that HBx facilitates the binding of *NF-κB* and *CREB* to *MAT2A* gene promoter. In addition, overexpression of *HBx* or *MAT2A* inhibits cell apoptosis, whereas knockdown of *MAT2A* expression stimulates apoptosis in hepatoma cells. Furthermore, we demonstrated that *HBx* reduces *MAT1A* expression and AdoMet production but enhances *MAT2β* expression. Thus, we proposed that *HBx* activates *MAT2A* expression through *NF-κB* and *CREB* signaling pathways to reduce AdoMet production, inhibit hepatoma cell apoptosis, and perhaps enhance HCC development. These findings should provide new insights into our understanding how the molecular mechanisms underline the effects of HBV infection on the production of MAT2A and the development of HCC.

Hepatitis B virus (HBV)[3] infection can cause severe liver diseases, including chronic hepatitis and hepatocellular carcinoma (HCC) (1). Such infection remains a major health problem with 2 billion people infected worldwide. Among them, 400 million are chronically infected (2). However, the complex mechanism by which HBV infection leads to the development of HCC mostly remains unclear.

It has been reported that the X protein (HBx) of HBV plays a crucial role in hepatocarcinogenesis (3). HBx is a multifunctional protein that activates many viral and cellular genes, modulates cellular signal transduction pathways, and regulates cell proliferation and apoptosis (4). Many studies have demonstrated that *HBx* regulates viral gene expression by transactivating the enhancers of HBV and also mediates the expression of cellular genes in infected cells to facilitate tumorigenesis (5–8). Several responsive elements are involved in the transactivation of *HBx*, including *AP-1*, *NF-κB*, and *HIF-1*. *HBx* also directly interacts with components of the basal transcription machinery, such as ribosome-binding protein 5, TATA-binding protein, and the transcriptional activator CREB/ATF to regulate gene expression (9–11). These interactions provide molecular mechanisms by which *HBx* regulates gene transcription, modulates cell proliferation and apoptosis, and stimulates the development of HBV-associated HCC.

Apoptosis plays an important role in the progress of liver diseases, because it goes through various extrinsic or intrinsic pathways with activation of caspases and the possible involvement of mitochondria alternation. Several reports have suggested that *HBx* can also regulate apoptotic pathways, provid-

* This work was supported by National Mega Project on Major Infectious Diseases Prevention and Treatment Research Grants 2008ZX10002-009 and 2009ZX10004-207, National Mega Project on Major Drug Development Research Grants 2009ZX09301-014 and 2011ZX09401-302, Major State Basic Research Development Program of China Research Grant 2005CB522901, National Science Foundation of China Research Grants 30730001 and 30872491, Program for Changjiang Scholars and Innovative Research Team in University Research Grant IRT0745, Key Project of Chinese Ministry of Education Research Grant 204114208, Department of Science and Technology of Hubei Province Research Grant 2005ABC003, Fundamental Research Funds for the Central Universities Research Grant 1102001, and Specialized Research Fund for the Doctoral Program of Higher Education Research Grant 20090141110033.

⌘ *Author's Choice*—Final version full access.

[1] To whom correspondence may be addressed. Tel.: 86-27-68713007; Fax: 86-27-87330795; E-mail: spss2005@126.com.

[2] To whom correspondence may be addressed. Tel.: 86-27-68754979; Fax: 86-27-68754592; E-mail: jwu@whu.edu.cn.

[3] The abbreviations used are: HBV, hepatitis B virus; AdoMet, *S*-adenosylmethionine; AdoHcy, *S*-adenosylhomocysteine; HCC, hepatocellular carcinoma; CREB, cAMP-response element-binding protein; nt, nucleotide; MAT, methionine adenosyltransferase; CRE, cAMP-response element.

ing additional potential mechanistic link between the function of *HBx* and the development of HBV-associated HCC (12, 13).

S-Adenosylmethionine (AdoMet), a principal biological methyl donor, is synthesized from methionine and ATP in a reaction catalyzed by methionine adenosyltransferase (MAT). In hepatocytes, the levels of AdoMet are high in quiescent and low in proliferating hepatocytes depending on the differentiation status of the cells (14). AdoMet not only controls liver growth but also regulates cell apoptosis, and its homeostasis in the liver influences MAT activities (15).

Two MAT-encoding genes (*MAT1A* and *MAT2A*) are found in the cells. *MAT1A* gene encodes for the α1 subunit, consisting of a dimer (MAT III) or a tetramer (MAT I), and is expressed in adult quiescent hepatocytes. *MAT2A* gene encodes for a catalytic subunit (α2), consisting of a native MAT isozyme (MAT II), and is expressed in proliferating liver, dedifferentiating cells, and cancer (15). MAT expression is switched from *MAT1A* to *MAT2A* during liver malignant transformation, and such alteration plays an important pathogenetic role in facilitating liver cancer growth (16–18).

Previous studies showed that activation of *MAT2A* expression stimulates the growth and inhibits apoptosis of cancer cells by changing AdoMet homeostasis (17, 19). *HBx* has been strongly implicated in tumor cell proliferation and apoptosis during hepatocarcinogenesis. This raised the question of whether HBV infection can activate the expression of *MAT2A*, resulting in the stimulation of tumor cell proliferation. However, the role of *HBx* in the transcription of *MAT2A* has not been investigated. In this study, we explored the possibility of a cross-talk between HBx and *MAT2A*, and we investigated the molecular mechanism underlying the effects of HBx on *MAT2A* expression and tumorigenesis. Our results demonstrated that *HBx* activated *MAT2A* expression through *NF-κB* and *CREB* signaling pathways, resulting in the decrease of AdoMet production and the inhibition of hepatoma cell apoptosis.

EXPERIMENTAL PROCEDURES

Patients and Tissue Specimens—Thirty seven cases of HBV-associated HCC were collected from Zhongnan Hospital, Wuhan University, between January 2008 and January 2009. No chemotherapy or radiation therapy was instituted before tumor excision. Both the tumors and corresponding peritumoral noncancerous tissues for each case were selected. All patients were tested positive for HBV surface antigen in serum. Matched normal human liver tissues were obtained from liver trauma patients undergoing partial hepatectomy. Informed consent in writing was obtained from each patient. The study protocol conformed to the ethical guidelines of the 1975 Declaration of Helsinki as reflected in *a priori* approval by the local ethics committee. No donor organs were obtained from executed prisoners or other institutionalized persons.

Immunohistochemistry—Representative tissues, including both HCC tissues and adjacent nontumorous liver tissues, were selected and sectioned in 4-μm thickness. The tissue samples were fixed by immersion in buffered formalin and embedded in paraffin according to standard procedures. Sections were processed in 0.05 M citrate buffer, pH 6.0, and heated in a microwave oven for 10 min for antigen retrieval. Sections were then incubated with the primary antibodies for 60 min at room temperature. All specimens stained for *HBx* and *MAT2A* were scored by two independent investigators who were blinded to the tested groups. *HBx* and *MAT2A* immunostainings were scored by the percentage of total cells that were positive in the cytoplasm. Slides were graded as follows: − (0–10% cells stained); + (10–50% cells stained); ++ (>50% cells stained).

Plasmid Construction and Cell Culture—A 986-bp promoter construct of the *MAT2A* gene, corresponding to the sequence from −951 to +35 (relative to the transcriptional start site) of the 5′-flanking region of the human *MAT2A* gene, was generated from human genomic DNA by PCR using F1 (5′-GAAGGTACCCACGGGGCAAGGACGGACTTGGGAG-3′) and R1 (5′-TCCACGCGTAACGCCTCGTGGAAGCCGTTGAGCT-3′) as forward and reverse primers carrying the KpnI and MluI sites at the 5′- and 3′-ends, respectively. The PCR product was cloned into KpnI and MluI sites of the pGL3-Basic vector. The resulting construct was confirmed by DNA sequencing. The 5′-flanking deletion constructs of the *MAT2A* promoters (−548/+35) *MAT2A*, (−320/+35) *MAT2A*, and (−108/+35) *MAT2A* were similarly generated by PCR using the (−951/+35) *MAT2A* construct as a template. The forward primers were F2 (5′-TCAGGTACCGCAGCACAAAACCTCCGCGATTCCC-3′), F3 (5′-GTAGGTACCGGTCTCTGGAGGGCCGGATTGCCAC-3′), and F4 (5′-TATGGTACCGCCGCCCGCCTGCTACGACTAGAAC-3′). Site-directed mutagenesis of two *NF-κB* sites and one *CREB* site was done by multiple rounds of PCR using the (−548/+35) MAT2A construct as a template and appropriate primers with altered bases. The primers used to make the *CREB* mutant were F5 (5′-AGAGCAATCCCCCgtaTCTCCTCGC-3′) and R2 (5′-GCAATCCGGCaCTCCAGAtACCGTT-3′). For mutating the *NF-κB1* site, the primers were F6 (5′-GGACGCtACCTCatGGAAgGCTATC-3′) and R3 (5′-AAAGCGACTGGaGCTTGgTGGACCC-3′). For mutating the *NF-κB2* site, the primers were F7 (5′-TAGCTGAAagGTCTCTGGAtGGCCG-3′) and R4 (5′-GCCCGGTATgTATAGAGCtGCGCCC-3′). The first two rounds of PCR generated two fragments of DNA, which were gel-purified and used as the templates for a third PCR with F2 and R1 primers. Single and double mutants were also ligated into the luciferase expression vector pGL3-Basic and verified by sequence analysis.

The cell lines, including the human normal liver cell line L02 and the hepatoma cell lines BEL-7404 and HepG2, were obtained from the Cell Bank of the Chinese Academy of Sciences (Shanghai, China). All cells were cultured in the recommended media supplemented with 10% (v/v) fetal bovine serum, 100 units/ml penicillin, and streptomycin at 37 °C in an incubator with 5% CO_2.

Transfection and Luciferase Reporter Assays—All transfections were performed using Lipofectamine 2000 reagent (Invitrogen) according to the manufacturer's protocol. For the luciferase assay, the cells were transiently co-transfected with the pRL-TK plasmid (Promega, Madison, WI) containing the *Renilla* luciferase gene, which is used for internal normalization, and various constructs containing different lengths of the *MAT2A* 5′-flanking region. After 48 h post-transfection, cell

lysates were prepared, and the luciferase activity was measured by using a luciferase assay system (Promega, Madison, WI). Cell lysates (10 μl) and luciferase assay substrates (100 μl) (Promega) were mixed, and fluorescence intensity was detected by a luminometer (Bio-Rad). Assays were performed in triplicate and expressed as means ± S.D. relative to vector control as 100%. All transfections were performed three times.

Western Blotting—Nuclear and cytoplasmic protein extracts were prepared from transfected cells and used for Western blot analysis using rabbit polyclonal antibodies. Protein (30 μg) from each sample was examined by SDS-10% PAGE and then electrotransferred to nitrocellulose membranes using a semi-dry transfer apparatus (Bio-Rad). Nitrocellulose membranes were subsequently subjected to Western blot analysis using the ECL Western blotting kit according to procedures described by the manufacturer (Amersham Biosciences).

MATII-specific Enzyme Activity Assay—MAT II-specific activity assays were performed as described previously (15). Protein extracts were obtained from transfected cells by sonication and then centrifugation at 13,000 × *g* for 15 min. Protein concentrations were determined by the Bradford method (see Ref. 18), and 250 μg was added to the reaction mixture containing 80 mM Tris-HCl, pH 7.4, 50 mM KCl, 40 mM $MgCl_2$, 5 mM ATP, 10 mM dithiothreitol, 0.5 mM EDTA, 50 μM methionine, and 0.3 μCi L-[*methyl*-^{3}H]methionine. The mixture was applied to a phosphocellulose paper disc (HA 0.45-μm, Millipore) and placed on a filtering system for washing. The disc was added to 10 ml of Scintiverse E for scintillation counting using a Beckman model LS6000TA liquid scintillation counter (Beckman Instruments, Fullerton, CA). MAT II activity was reported as nanomoles of AdoMet formed per mg of protein/40 min. AdoMet and AdoHcy contents were determined by reverse phase-HPLC, as described previously (19).

Quantification of the Levels of AdoMet and AdoHcy by HPLC—AdoMet and AdoHcy contents were determined by reverse phase-HPLC, as described previously (19). The AdoMet and AdoHcy standards were dissolved in distal water at a concentration of 1 mmol/liter and then diluted with 0.4 mol/liter of $HClO_4$ to the final concentrations used for HPLC analysis. 25 μl of standard solution containing 50–11,000 pmol was injected into HPLC for preparation of standard curve. The homogenate was centrifuged at 1,000 × *g* for 5 min (Beckman glycoprotein receptor centrifuge). The pellet was resuspended in 0.5 M perchloric acid and centrifuged at 1,000 × *g* for 15 min. The aqueous layer was quantitatively removed and neutralized with 3 M KOH. AdoMet and AdoHcy were determined in the neutralized perchloric acid extracts by HPLC (series 410 LC pump, PerkinElmer Life Sciences) with an LC-90 UV detector and an LC-100 integrator (PerkinElmer Life Sciences) using a Partisil SCX 10-μm column (25 × 0.44-cm inner diameter; Whatman). AdoMet and AdoHcy were identified by measuring absorbance at 254 nm at a sensitivity scale of 0.01. The amount of AdoMet and AdoHcy in each sample was calculated from standard curves of AdoMet and AdoHcy prepared at the same time as the samples. The identity of AdoMet and AdoHcy peaks was also confirmed by comparison of the sample with known standards.

Electrophoresis Mobility Shift Assay (EMSA)—Nuclear extracts were prepared from HepG2 cells. Probes were generated by annealing single strand oligonucleotides containing the cognate promoter regions of the *MAT2A* gene and labeling the ends with [γ-^{32}P]ATP using T4 polynucleotide kinase (Takara). For the CREB site, the oligonucleotide sequences were 5′-AGAGCAATCCCCCACGTCTCCTCGC-3′ and 5′-GCGAGGAGACGTGGGGGATTGCTCT-3′. For the *NF-κB2* site, the oligonucleotide sequences were 5′-TCTGGAGGGCCGGATTGCCACGGCA-3′ and 5′-TG CCGTGGCAATCCGGCCCTCCAGA-3′. The *MAT2A cis*-regulatory motifs of *CREB* and *NF-κB2* were analyzed. EMSAs were performed with 4 μg of nuclear extract in binding buffer (20 mM Hepes, pH 7.9, 0.1 mM EDTA, pH 8.0, 75 mM KCl, 2.5 mM $MgCl_2$, and 1 mM DTT) containing 1 μg of poly(dI-dC). To ensure the specific binding of transcription factors to the probe, unlabeled double-stranded oligonucleotide competitors were preincubated at a 50-fold molar excess for 10 min prior to probe addition. For supershift experiments, 2 μg of purified polyclonal antibody directed against *NF-κB* subunit *p65* (anti-p65), *CREB* (anti-CREB), or IgG was incubated with nuclear extracts on ice for 30 min before being added to the binding buffer. Samples were then separated by electrophoresis on 5% nondenaturing polyacrylamide, 0.25× Tris borate/EDTA (TBE) gels, and the gels were dried and subjected to autoradiography.

Chromatin Immunoprecipitation Assay (ChIP)—HepG2 cells were transfected with relevant plasmids and then cross-linked using 1% formaldehyde at 37 °C for 10 min. After washing with PBS, cells were resuspended in 300 μl of lysis buffer (50 mM Tris, pH 8.1, 10 mM EDTA, 1% SDS, 1 mM PMSF). DNA was sheared to small fragments by sonication. The supernatants were pre-cleared using herring sperm DNA/protein G-Sepharose slurry (Sigma). The recovered supernatants were incubated with antibody directed against *NF-κB2* (anti-p50, p65, p52, and RelB) and *CREB* (anti-CREB1 and CREB2) or an isotype control IgG for 2 h in the presence of herring sperm DNA and protein G-Sepharose beads. The immunoprecipitated DNA was retrieved from the beads with 1% SDS and 1.1 M $NaHCO_3$ solution at 65 °C for 6 h. DNA was then purified using a PCR purification kit (Qiagen), and PCR was done on the extracted DNA using *MAT2A* promoter-specific primers. For Chip1, the primer was 5′-GGACGCGACCTCCGGGAAAGCTATC-3′ and 5′-GAGCTAGGAGAAAAATGCAGACGCG-3′. For Chip2, the primer was 5′-GATAGCTGAACGGTCTCTGGAGGGC-3′ and 5′-CGGAGTCCGGGCTGAACCACACTGC-3′.

Statistical Analysis—The data have been presented as the mean ± S.D. The significance of the differences was determined by Student's *t* test. The correlations between the expression of *HBx* and *MAT2A* were analyzed by χ^2 test or Fisher exact test. Spearman rank correlation test was used to determine correlations between the variables. Differences were considered statistically significant for $p < 0.05$. All statistical analyses were performed using professional statistical software (SPSS 15.0 for Windows, SPSS Inc., Chicago).

RESULTS

MAT2A Expression Is Correlated with HBx Expression in Liver Cancer Tissues—The expression status of *MAT2A* and *HBx* was examined by immunohistochemical staining of 37

TABLE 1

Expression status of HBx and MAT2A in HBV-associated liver tumor tissues and the corresponding peritumoral tissues

Tumor volume (cm^3) was calculated by the formula: length (cm) × shortest width (cm) × longest width (cm), in which length was the longest axis. Immunohistochemical staining was estimated as follows: − (0–10% cells stained), + (10–50% cells stained), ++ (>50% cells stained).

							Immunohistochemical staining			
							HBx		MAT2A	
Case	Age	Sex	Tumor size	Nodule no.	Etiology	Edmonson grade	Peritumoral tissues	Tumor tissues	Peritumoral tissues	Tumor tissues
			cm^3							
1	43	M	1125.3	6	HBV	IV	++	++	+	++
2	61	M	154.7	1	HBV	I	−	+	+	++
3	49	M	564.7	3	HBV	III	+	++	++	++
4	39	F	86.9	1	HBV	I	−	−	−	+
5	54	M	121.4	2	HBV	III	−	++	+	++
6	43	M	128.2	0	HBV	II	−	−	−	+
7	57	F	236.7	5	HBV	III	++	++	++	++
8	57	M	251.8	4	HBV	II	+	++	+	+
9	62	M	345.4	7	HBV	III	−	+	−	+
10	37	M	548.3	6	HBV	III	−	++	+	++
11	45	F	784.5	4	HBV	IV	+	++	+	++
12	61	M	113.4	0	HBV	I	−	+	−	+
13	66	M	421.7	2	HBV	II	+	++	+	+
14	50	M	65.9	0	HBV	III	−	+	−	+
15	42	M	1545.6	8	HBV	II	+	+	+	++
16	70	F	218.4	3	HBV	IV	−	+	−	+
17	53	M	147.8	1	HBV	II	+	+	+	++
18	49	M	824.3	3	HBV	III	−	++	+	++
19	56	M	245.8	4	HBV	III	++	++	++	++
20	61	F	310.5	2	HBV	IV	−	++	−	++
21	45	M	128.6	0	HBV	II	−	+	−	+
22	59	M	574.2	5	HBV	III	−	++	+	++
23	47	M	315.4	2	HBV	IV	+	++	−	++
24	65	F	519.3	3	HBV	II	−	+	−	+
25	36	M	62.7	0	HBV	I	−	+	−	+
26	54	M	193.1	2	HBV	II	+	++	+	++
27	58	M	371.2	4	HBV	IV	−	+	+	++
28	51	F	87.3	0	HBV	II	−	++	++	++
29	60	M	245.3	2	HBV	III	+	+	−	+
30	45	M	118.3	2	HBV	II	−	+	+	++
31	52	M	149.4	1	HBV	III	−	+	−	+
32	64	F	368.7	5	HBV	I	+	+	+	+
33	57	M	294.7	2	HBV	III	+	++	++	+
34	46	F	143.1	3	HBV	III	−	++	+	++
35	63	M	244.8	6	HBV	II	+	+	−	+
36	48	M	129.3	4	HBV	III	+	++	−	++
37	60	M	954.6	8	HBV	IV	++	++	++	++

pairs of HBV-associated liver tumor tissues/corresponding peritumoral tissues using antibodies to *HBx* and *MAT2A*, respectively (Table 1). Results showed that MAT2A was not detected in normal liver tissue (Fig. 1*A, panel a*), expressed at high level in HBV-associated liver tumor tissues (Fig. 1*A, panel b*), and produced at a lower level in the corresponding peritumoral tissues (Fig. 1*A, panel c*). Similarly, *HBx* was not detected in normal liver tissues (Fig. 1*A, panel d*), expressed at high level in liver tumor tissues (Fig. 1*A, panel e*), and produced at lower level in peritumoral tissues (Fig. 1*A, panel f*).

The potential correlation between the expression statuses of *MAT2A* and *HBx* was further analyzed (Table 1 and Fig. 1*B*). Results indicated that among the 19 liver tumor tissues with high levels of *HBx*, most (16) of them (84.2%) expressed high levels of *MAT2A*, and the remaining 3 (15.8%) expressed low levels of *MAT2A*. However, among the 16 liver tumor tissues with low levels of *HBx*, most (11) of them (68.7%) expressed low levels of MAT2A, and the remaining 5 (31.3%) expressed high levels of MAT2A. In addition, in the two cancer tissues with no detectable HBx, *MAT2A* was also expressed at low level. These results demonstrated that there is a correlation between *HBx* expression and *MAT2A* expression with a statistical significance ($p = 0.0074$, χ^2 test; $p = 0.0058$, Fisher two-tailed exact tests).

To further confirm the expression status of *MAT2A* and HBx, seven liver tumor tissues (samples 1–7) were selected for Western blot analyses using antibodies to the two proteins, respectively (Fig. 1*C*). Results indicated that *MAT2A* was detected at a high level in liver tumor tissues with high level of HBx (Fig. 1*C*, *lanes 1–3, 5,* and *7*) and detected at low level in liver tumor tissues with lower level of HBx (Fig. 1*C*, *lanes 4* and *6*). These results further demonstrated that a correlation indeed exists between *HBx* expression and *MAT2A* expression in liver tumor tissues.

HBx Induces MAT2A Expression and Enhances MAT II Enzyme Activity—To determine the effects of HBV on the expression of *MAT2A*, the levels of *MAT2A* mRNA and MAT II protein were detected in HepG2 and HepG2.2.15 cells by RT-PCR and Western blot analyses, respectively. Results showed that the levels of *MAT2A* mRNA (Fig. 2*A*) and MAT II protein (Fig. 2*B*) were higher in HepG2.2.15 cells than that in HepG2 cells. Because HepG2.2.15 cells, but not HepG2 cells, carry an integrated HBV genomic DNA on its chromosome, it is reasonable to believe that HBV was responsible for the enhanced expression of the *MAT2A* gene in HepG2.2.15 cells.

The role of HBV in the regulation of MAT II enzyme activity was also determined by transfecting HepG2 cells with plasmid (pBlue-HBV containing 1.3-fold HBV genome) or control plas-

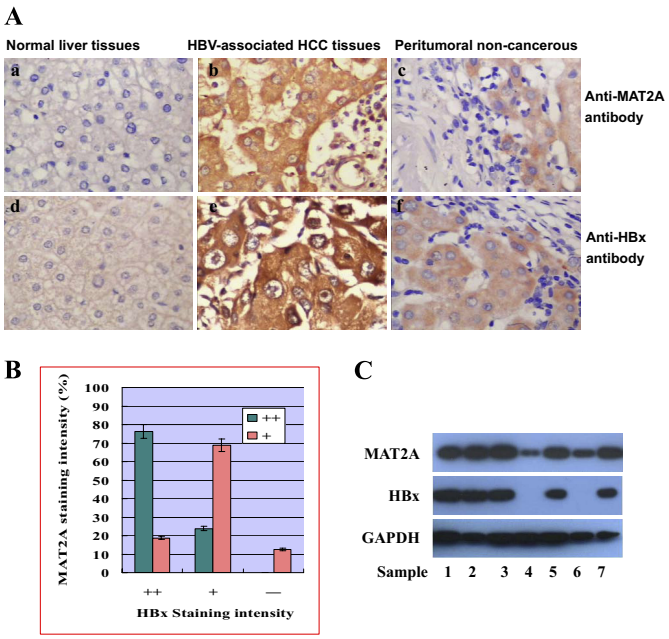

FIGURE 1. **Determination of expression status of MAT2A and HBx in HBV-associated liver tumor tissues by immunohistochemistry analyses.** *A,* representative results of immunohistochemistry analyses of 37 cases of surgically resected HBV-associated HCC tissues and their adjacent nontumorous liver tissues. *Panels a* and *d,* normal liver tissues obtained from liver traumas patients undergoing partial hepatectomy; *panels b* and *e,* HBV-associated HCC tissues; *panels c* and *f,* peritumoral noncancerous tissues. *Panels a–c,* immunohistochemistry analyses using antibody to *MAT2A*; *panels d–f,* immunohistochemistry analyses using antibody to *HBx*. *B,* analyses of the correlation between the expression level of *MAT2A* and *HBx*. The levels (high ++; low +; and undetectable −) of *HBx* in HBV-associated HCC tissues were compared with that of MAT2A, respectively ($p = 0.0075$, χ^2 test; $p = 0.0061$, Fisher two-tailed exact test). *C,* seven HBV-associated HCC tissues (*samples 1–7*) were selected for Western blot analyses using antibodies to MAT2A, HBx, and GAPDH proteins, respectively.

mid (its parental plasmid pBlue-SK), and then MAT II activity was measured at different times after transfection. Results showed that MAT II activities were significantly higher in cells transfected with pBlue-HBV than in untransfected cells or in cells transfected with pBlue-SK (Fig. 2*C*).

Next, we would like to find out the effects of individual proteins of HBV on the activation of *MAT2A* expression. HepG2 cells were co-transfected with plasmid pGL3-*MAT2A*, in which the expression of luciferase gene was under the control of *MAT2A* gene promoter, along with plasmids (pcDNA-S, pcDNA-preS1, pcDNA-preS2, pcDNA-HBE, pcDNA-HBc, pcDNA-HBx, and pcDNA-HBp) carrying individual genes of HBV or control plasmid, respectively. Results from luciferase activity assays showed that *MAT2A* promoter activity was significantly stimulated by *HBx* but not by the rest of proteins of HBV (Fig. 2*D*).

To determine the specificity of *HBx* in the activation of the *MAT2A* gene promoter, HepG2 cells were co-transfected with pGL3-MAT2A and pcDNA-HBx at different concentrations. Results indicated that the levels of luciferase activities increased as the concentrations of pcDNA-HBx increased (Fig. 2*E*). To evaluate the expression status of *HBx* in transfected cells, proteins were detected by Western blots using antibodies to *HBx* or *GAPDH* (as a control). Results showed that the levels of HBx protein increased as the concentrations of pcDNA-HBx increased in transfected cells, although levels of *GAPDH* remained relatively unchanged (Fig. 2*E*). These results suggested that *HBx* activated *MAT2A* expression in a dose-dependent manner.

The roles of individual proteins of HBV in the regulation of MAT II enzyme activity were evaluated. HepG2 cells were transfected with plasmids carrying each of the HBV genes or the control plasmid pcDNA-3.1, respectively. Results from MAT II activity analyses indicated that the enzyme activity was stimulated only by HBx, but not by the rest of viral proteins S, preS1, preS2, HBe, HBc, or P (Fig. 2*F*).

MAT2A Gene Is Expressed in Hepatoma Cell Lines and Enhanced by HBx—To investigate the relevance of *MAT2A* in hepatoma development, the expression levels of the endogenous *MAT2A* gene were determined in normal hepatic cell lines and hepatoma cell lines by RT-PCR and Western blot analyses, respectively. Results showed that *MAT2A* mRNA (Fig. 3*A*) and its protein (Fig. 3*B*) were detected in the two hepatoma cell lines (HepG2 and BEL7404) but not in the normal hepatic cell line (L02), indicating *MAT2A* gene was expressed specifically in hepatoma cells.

The role of *HBx* in the regulation of *MAT2A* expression was then analyzed by measuring its effect on the activity of the MAT II enzyme in L02, HepG2, and BEL-7404 cell lines, respectively. Cells from the three cell lines were transfected with plasmid pcDNA-HBx at different concentrations. Results showed that HBx enhanced MAT II activity in all three cell lines (Fig. 3*C*). To evaluate the expression status of HBx in transfected cells, proteins were detected by Western blots using antibody to HBx or to GAPDH. Results showed that the levels of HBx protein were increased as the concentrations of pcDNA-HBx increased in transfected cells, although levels of GAPDH remained relatively unchanged (Fig. 3*C*). These results demonstrated that HBx induced MAT II enzyme activity in a dose-dependent manner in all three cell lines.

NF-κB and CRE Binding Elements Are Required for HBx-activated MAT2A Expression—To define the roles of *cis*-regulatory elements of *MAT2A* promoter in response to *HBx* regulation, a series of truncated mutants of *MAT2A* promoter were generated (Fig. 4*A*, *left panel*). To test the functions of these mutated *MAT2A* promoters, HepG2 and BEL7404 cells were co-transfected with pcDNA-*HBx* along with plasmids containing the luciferase reporter gene under the control of wild-type and truncated *MAT2A* promoters. Results from luciferase activity assays indicated that deletion from nt −951 to −548 had no effect on HBx-induced *MAT2A* promoter activity, and deletion from nt −951 to −320 reduced *HBx*-mediated *MAT2A* promoter activity, and deletion from nt −951 to −108 eliminated HBx function in the induction of MAT2A (Fig. 4*A*, *right panel*). These results suggested that the sequence between nt −548 and −108 was critical for the activation of *MAT2A* promoter regulated by *HBx*.

Analyses of the cis-regulatory elements on the *MAT2A* promoter revealed two *NF-κB*-binding sites (*NF-κB1* and *NF-κB2*) and one *CRE*-binding site (CREB) in this region. To evaluate the roles of these regulatory elements in the activation of the *MAT2A* promoter regulated by *HBx*, these *cis*-regulatory elements were altered by site-directed mutagenesis, respectively

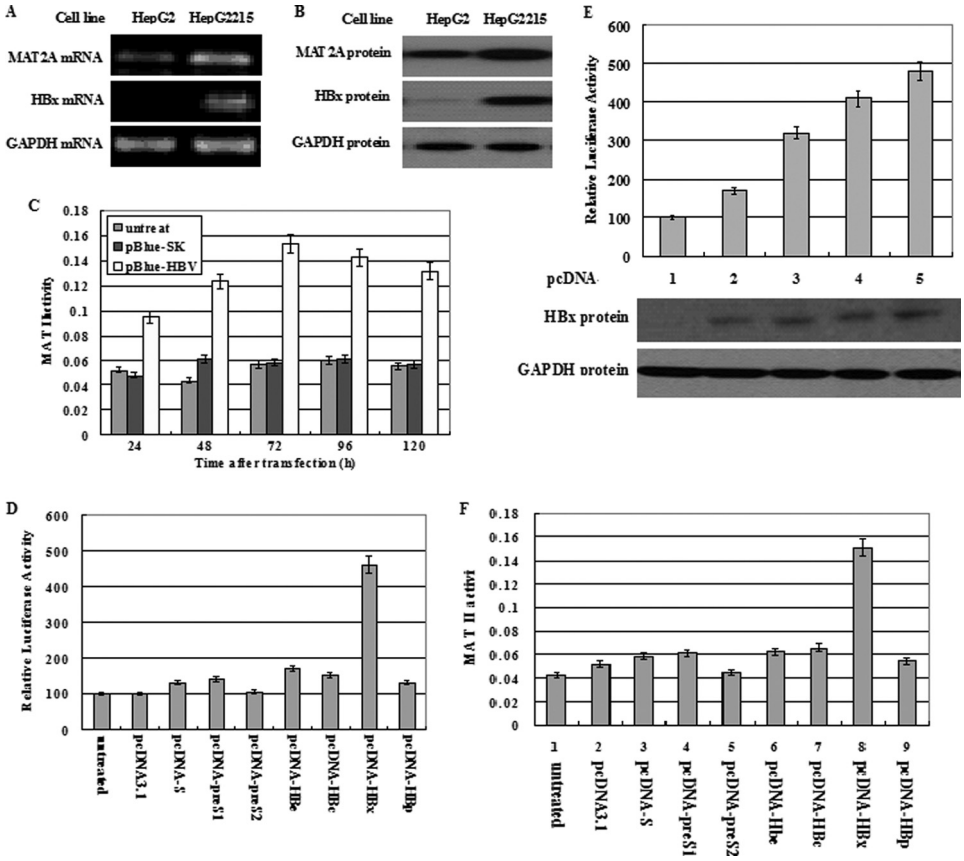

FIGURE 2. **Role of *HBx* in the regulation of *MAT2A* expression in hepatoma cells.** *A,* RT-PCR analyses of mRNA levels in HepG2 and HepG2.2.15 cells using primers specific to the *MAT2A, HBx,* and *GAPDH* genes, respectively. *B,* Western blot analyses of protein expression status in HepG2 and HepG2.2.15 cells using antibodies to MAT2A, HBx, and GAPDH proteins, respectively. *C,* HepG2 cells were transfected with pBlue-SK or pBlue-HBV, respectively, at different times as indicated. MAT II enzyme activities were determined. *D,* HepG2 cells were co-transfected with a reporter plasmid pGL3-MAT2A, in which the luciferase gene is under the control of the *MAT2A* promoter, along with plasmids (pcDNA-S, pcDNA-preS1, pcDNA-preS2, pcDNA-HBs, pcDNA-HBx, and pcDNA-HBp) expressing each of the HBV proteins, respectively. Relative luciferase activity was determined by standard procedures. Results shown are mean ± S.D. of three experiments performed in duplicate. *E,* HepG2 cells were co-transfected with the reporter plasmid pGL3-MAT2A and pcDNA-HBx at different concentrations. Relative luciferase activity was determined by standard procedures. Results shown are mean ± S.D. of three experiments performed in duplicate. The protein levels were determined by Western blot using antibodies to HBx and GAPDH, respectively. *F,* HepG2 cells were transfected with pcDNA3.1 or plasmids expressing each of the HBV proteins, respectively. MAT II enzyme activities were determined 48 h post-transfection.

(Fig. 4*B*, *left panel*). Results from luciferase activity assays showed that *NF-κB1* mutation had no effect on *HBx*-induced *MAT2A* promoter activity, whereas *NF-κB2* or *CREB* mutations significantly reduced the *MAT2A* promoter activity regulated by *HBx* (Fig. 4*B*, *right panel*). These results suggested that *NF-κB2* and *CREB* recognition elements are required for the activation of *MAT2A* expression mediated by *HBx*.

HBx Facilitates the Binding of CREB and NF-κB to the MAT2A Promoter—Because *CREB* and *NF-κB2* regulatory elements are required for the activation of *MAT2A* expression mediated by *HBx*, it is reasonable to assume that *HBx* may enhance the binding of *CREB* and *NF-κB* to the *MAT2A* promoter. To confirm this speculation, electrophoresis mobility shift assays (EMSA) were performed. HepG2 cells were transfected with pcDNA-HBx at different concentrations (Fig. 5, *A* and *B*, *lanes 2–7*) or with the control plasmid (Fig. 5, *A* and *B*, *lane 1*). The nuclear extracts were prepared from transfected cells and incubated with the [^{32}P]DNA probe. To ensure the specific binding of transcription factors to the probe, mutated oligonucleotide (Fig. 5, *A* and *B*, *lane 5*), nonspecific competitor (Fig. 5, *A* and *B*, *lane 6*), and unlabeled double-stranded oligonucleotide competitor (Fig. 5, *A* and *B*, *lane 7*) were added prior to the addition of labeled probe. To determine the specific binding of *NF-κB* and *CREB* to the promoter, polyclonal antibodies to *NF-κB* (anti-p65) (Fig. 5*A*, *lane 4*) or *CREB* (anti-CREB) (Fig. 5*B*, *lane 4*) were incubated with nuclear extracts before adding the binding buffer, respectively. DNA probes used in this study contained either the *CREB* element (Fig. 5*A*) or the *NF-κB2* element (Fig. 5*B*) of the *MAT2A* promoter.

Results from EMSA using the CREB probe showed that one faint band of protein-DNA complex (shift band) was detected in the absence of *HBx* (Fig. 5*A*, *lane 1*), but the shift bands were enhanced in the presence of *HBx,* and the level of shift band increased as the concentration of *HBx* increased (Fig. 5*A*, *lanes 2* and *3*). Moreover, the shift band was eliminated in the presence of mutated oligonucleotide (Fig. 5*A*, *lane 5*) and unlabeled double-stranded oligonucleotide competitor (Fig. 5*A*, *lane 7*) but was not affected by nonspecific competitor (Fig. 5*A*, *lane 6*). In addition, a specific protein-DNA complex (supershift band) was detected in the presence of anti-CREB antibody (Fig. 5*A*, *lane 4*).

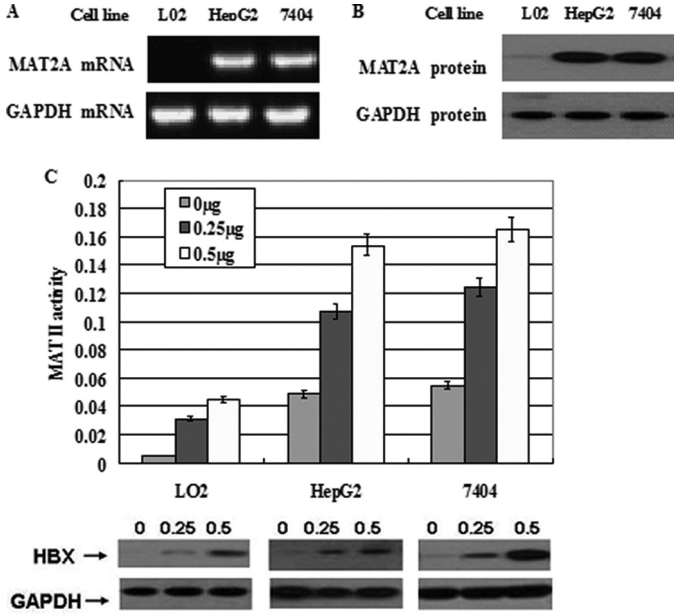

FIGURE 3. **Determination of *MAT2A* expression levels and MAT II activities regulated by *HBx*.** *A,* RT-PCR analyses of mRNA levels in L02, HepG2, and BEL7404 cells using primers specific to the *MAT2A* or *GAPDH* gene. *B,* Western blot analyses of protein levels in L02, HepG2, and BEL7404 cells using antibodies to MAT2A or GAPDH proteins. *C,* L02, HepG2, and BEL7404 cells were transfected with pcDNA-HBx at 0, 0.25, and 0.5 μg per well. MAT II enzyme activity was measured 48 h post-transfection. Data are shown as the mean ± S.D. of three independent experiments. The expression status of HBx and GAPDH was also determined using antibodies to the two proteins, respectively.

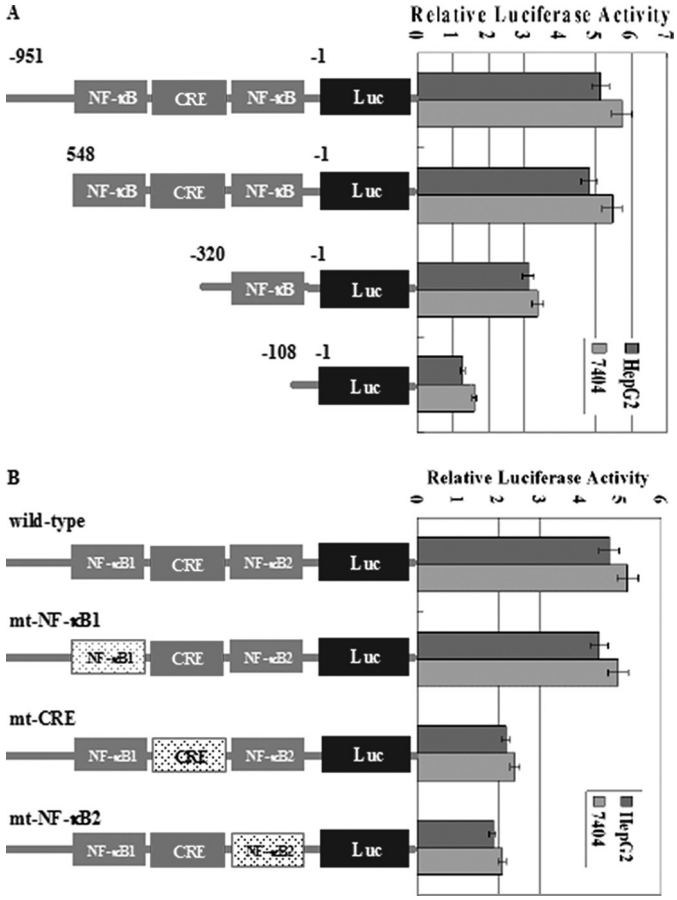

FIGURE 4. **Requirement of *cis*-acting elements in the activation of *MAT2A* gene expression regulated by *HBx*.** *A, left panel,* diagrams of reporter constructs containing the luciferase (*Luc*) gene under the control of the human *MAT2A* promoter or its serial deletions. *A, right panel,* HepG2 and BEL-7404 cell lines were co-transfected with pcDNA-HBx along with the constructed reporter plasmids with wild-type or mutated *MAT2A* promoters. Relative luciferase activity was determined. The results shown are the means ± S.D. of three experiments performed in duplicate. *B, left panel,* diagrams of reporter constructs containing the luciferase gene under the control of *MAT2A* promoter with specific mutations in *cis*-regulatory elements as indicated. *B, right panel,* HepG2 and BEL-7404 cell lines were co-transfected with pcDNA-HBx along with these constructed reporter plasmids with wild-type or mutated *MAT2A* promoters. Relative luciferase activity was determined. The results shown are the means ± S.D. of three experiments performed in duplicate.

Similar results were observed when the *NF-κB2* probe was used. EMSA results showed that the protein-DNA complex (shift band) was enhanced in the presence of HBx (Fig. 5*B*, *lanes 2* and *3*), although it was reduced in the presence of mutated oligonucleotide (Fig. 5*B*, *lane 5*) and unlabeled double-stranded oligonucleotide competitor (Fig. 5*B*, *lane 7*), but it did not affect the nonspecific competitor (Fig. 5*B*, *lane 6*). Again, a specific protein-DNA complex (supershift band) was detected in the presence of the anti-CREB antibody (Fig. 5*B*, *lane 4*).

The roles of *HBx* in facilitating the binding of *NF-κB* and *CREB* to the *MAT2A* promoter *in vivo* were further confirmed by ChIP assays. Chromatin fragments were prepared from HepG2 cells transfected with pcDNA-HBx and immunoprecipitated with antibodies against either *NF-κB* (*p50, p65, p52,* and *RelB*) or *CREB* (*CREB1* and *CREB2*), respectively. The locations of the PCR products are indicated as Chip1 and Chip2 under the simplified genomic structures of the *MAT2A* promoter (Fig. 5*C*). Results of Chip1 showed that PCR products were only produced from DNA isolated from cells transfected with pcDNA-HBx in the presence of antibodies to *CREB1* and to *CREB2* but not detected in the presence of control plasmids and antibody to p50, p65, p52, or to RelB (Fig. 5*C*, *left panel*). Results of Chip2 showed that PCR products were only detected from DNA isolated from cells transfected with pcDNA-HBx in the presence of antibodies to *p50, p65, p52,* or to *RelB* but were not detected in the presence of control plasmids and antibodies to *CREB1* or to *CREB2*. These results indicated that *HBx* enhanced the binding of *CREB* and *NF-κB* to the *CREB* and *NF-κB2* recognition sites in the *MAT2A* promoter, respectively.

NF-κB and CREB Pathways Are Involved in HBx-regulated MAT2A Expression—The roles of *NF-κB* and *CREB* signal transduction pathways in the activation of *MAT2A* expression regulated by *HBx* in hepatoma cells were further evaluated. Inhibitors of the signaling components, including MG132 (inhibitor of NF-κB), PD098059 (inhibitor of ERK), U0126 (inhibitor of MEK1/2), H89 (inhibitor of PKA), SP600125 (inhibitor of JNK MAPK), GF109203 (inhibitor of PKC), LY294002 (inhibitor of PI3K), and SB203580 (inhibitor of p38), were added to the cells transfected with pcDNA-HBx for the screening of the signaling pathway(s) involved in the HBx-activated *MAT2A* expression. MAT II enzyme activities and MAT2A protein levels were determined 72 h post-transfection. Results indicated that both MAT II activities and MAT2A protein levels activated by HBx were significantly reduced in the presence of inhibitors, MG132, PD098095, U0126, GF109203, LY294002, and SB203580, indicating signaling components, *PI3K, MEK1/2,* p38

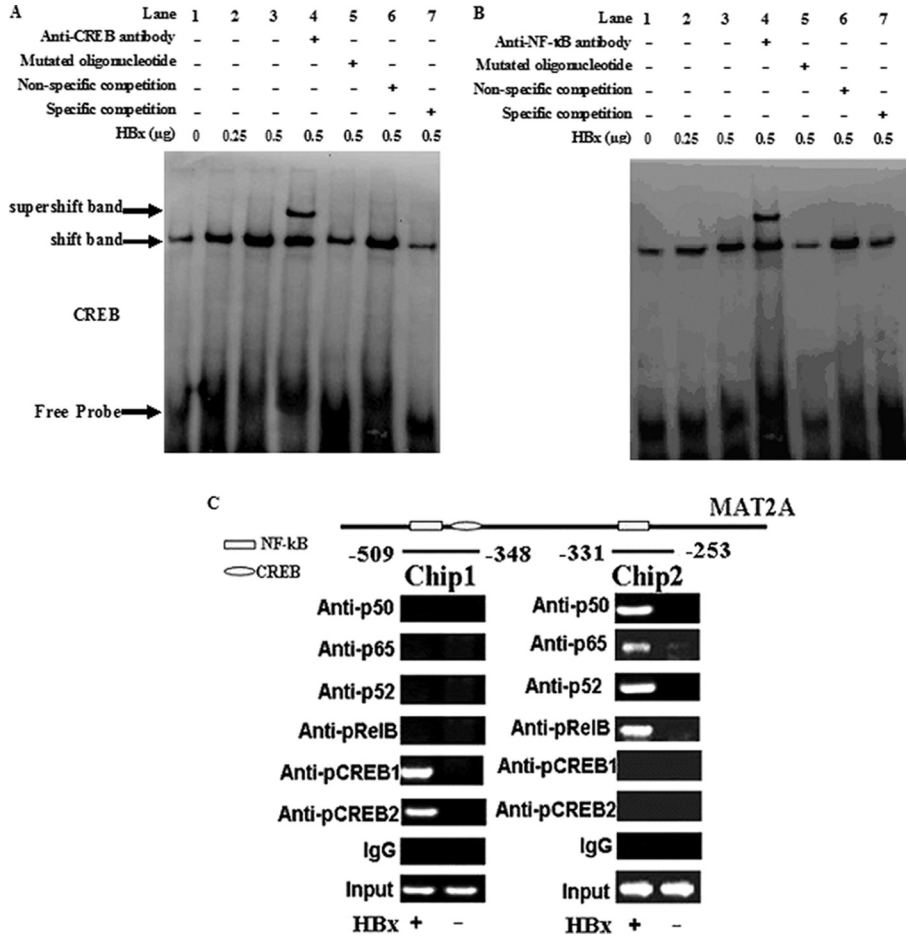

FIGURE 5. **Analyses of effects of *HBx* on binding of *CREB* and *NF-κB* to the *MAT2A* promoter.** *A,* analyses of the effect of *HBx* on the binding of *CREB* to the *MAT2A* promoter by EMSA. EMSA was performed with nuclear extracts of HepG2 cells transfected with control plasmid (*lane 1*) or pcDNA-HBx at different concentrations (*lanes 2–7*). *CREB* probe was generated by annealing single-stranded and end-labeled oligonucleotides containing the cognate *MAT2A* promoter region (nucleotides −385/−365). Mutated oligonucleotide (*lane 2*), nonspecific competitor (*lane 6*), or specific competitor (unlabeled CREB probe, *lane 7*) were used as a control. For supershift, antibody to CREB (*lane 4*) was incubated with nuclear extracts before being added to the reaction. *B,* analyses of the effect of *HBx* on the binding of *NF-κB* to the *MAT2A* promoter by EMSA. EMSA was performed with nuclear extracts of HepG2 cells transfected with pcDNA-HBx. *NF-κB* probe was generated by annealing single-stranded and end-labeled oligonucleotides containing the cognate *MAT2A* promoter region (nucleotides −296/−284). Mutated oligonucleotide (*lane 2*), nonspecific competitor (*lane 6*), or specific competitor (unlabeled *NF-κB* probe, *lane 7*) were used as a control. For supershift, antibody to *p65* (*lane 4*) was incubated with nuclear extracts before being added to the reaction. Samples were electrophoresed on 5% nondenaturing polyacrylamide gels and visualized by autoradiography. *Arrows* indicate the shift bands or supershifted protein-DNA complexes or free probes. *C,* determination of the role of *HBx* in the binding of *CREB* and *NF-κB* to the *MAT2A* promoter by ChIP assays. HepG2 cells transfected with pcDNA-HBx (+) or control vector (−) were lysed and subjected to ChIP assays. The exact locations of PCR products of Chip1 and Chip2 underlie the simplified genomic structures of the *MAT2A* gene promoter. The results are representatives of four independent experiments.

MAPK, ERK, PKC, and *NF-κB* were involved in HBx-enhanced MAT2A protein expression (Fig. 6*A*).

To confirm whether the effects of inhibitors on *MAT2A* expression were specific to *HBx*, HepG2 cells not transfected with the HBx expression plasmid were treated with these inhibitors. Results showed that MAT II enzyme activities and protein levels were not affected by the treatment of SP600125 (JNK MAPK), H89 (PKA), and PD098095 (ERK), were slightly reduced by the treatment of LY294002 (PI3K), U0126 (MEK1/2), and GF109203 (PKC), and were reduced by the treatment of MG132 (NF-κB) and SB203580 (p38), but such reductions caused by MG132 and SB203580 were not significant (Fig. 6*B*), indicating ERK, MEK1/2, PKC, and PI3K were not involved in the activation of *MAT2A* expression, whereas the endogenous NF-κB and p38 had slightly affects on such activation. Taken together, the above results demonstrated that the effects of those inhibitors of signaling pathways on MAT II protein expression were specific to HBx.

The roles of *NF-κB* and *CREB* signal transduction pathways in the activation of *MAT2A* expression regulated by *HBx* in hepatoma cells were also evaluated by the approaches of RNA interference. Cells were transfected with pGL3-MAT2A and pcDNA-HBx and treated with shRNA specific to the signaling components. Results showed that HBx-activated *MAT2A* promoter activity was reduced in the presence of shRNA specific to *RIG-I, MAVS, IRAK2, TRAF6, IKKα, IKKβ, IKKi, p50,* and *p65,* respectively (Fig. 6*C*).

We also demonstrated that MAT II activity (Fig. 6*D*, *top panel*) and the *MAT2A* mRNA level (Fig. 6*D*, *lower panel*) were reduced by the inhibitor of *NF-κB* (MG132) in a dose-dependent fashion. In addition, MAT II activity (Fig. 6*E*, *top panel*) and the *MAT2A* mRNA level (Fig. 6*E*, *lower panel*) were also reduced by shRNA to

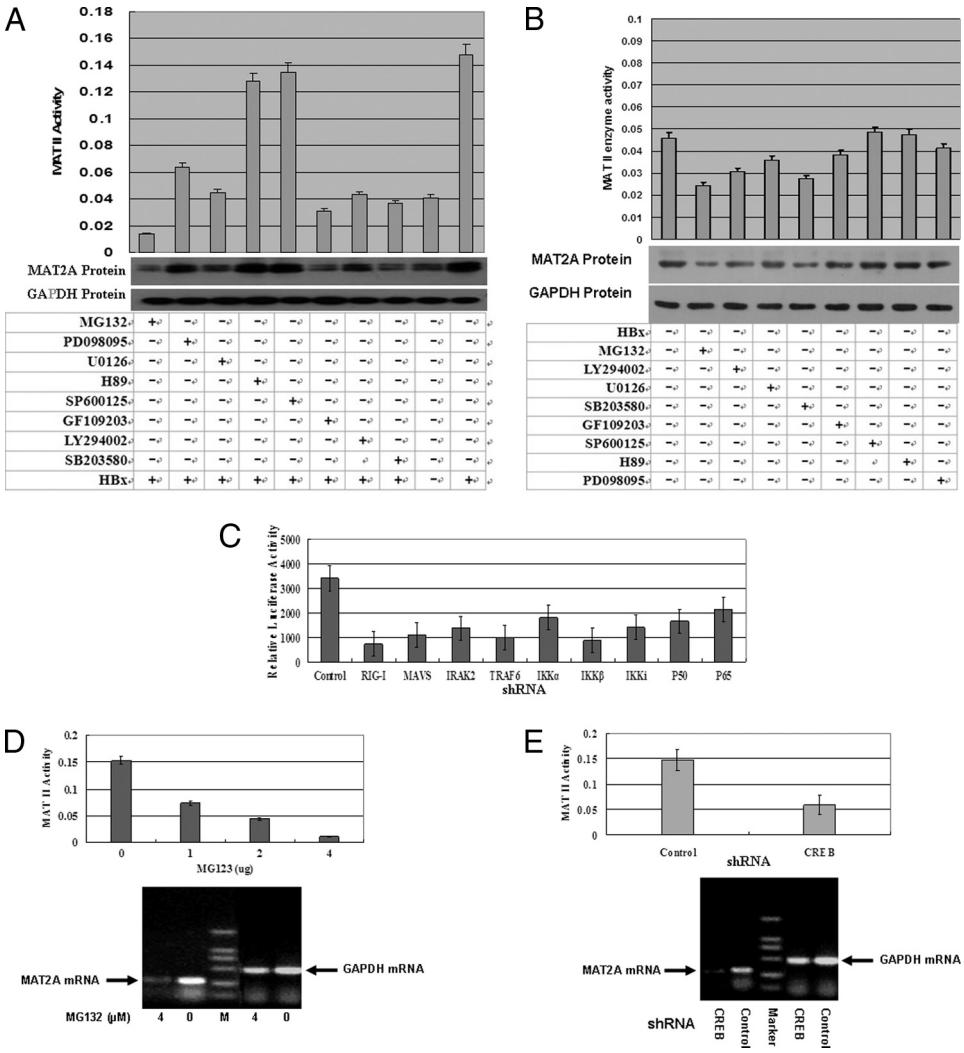

FIGURE 6. **Determination of signaling pathways involved in the activation of *MAT2A* gene expression regulated by *HBx*.** *A,* analyses of the effects of inhibitors of signaling components on the activation of *MAT2A* expression regulated by HBx. HepG2 cells were transfected with pcDNA-HBx and treated with LY294002 (10 μM), U0126 (13 μM), MG132 (4 μM), SB203580 (10 μM), GF109203 (1 μM), H89 (10 μM), SP600125 (30 μM), and PD098059 (10 μM), respectively. MAT II enzyme activity was measured, and MAT2A protein was determined by Western blot analyses 72 h post-transfection. *B,* HepG2 cells were transfected with pcDNA and treated with LY294002 (10 μM), U0126 (13 μM), MG132 (4 μM), SB203580 (10 μM), GF109203 (1 μM), H89 (10 μM), SP600125 (30 μM), and PD098059 (10 μM), respectively. MAT II enzyme activity was measured and MAT2A protein was determined by Western blot analyses 72 h post-transfection. *C,* determination of the effects of shRNAs of signaling components on the activation of *MAT2A* expression regulated by HBx. HepG2 cells were co-transfected with pMAT2A-Luc and pcDNA-HBx along with plasmids expressing shRNA-control, shRNA-RIG-I, shRNA-MAV, shRNA-IRAK2, shRNA-TRAF6, shRNA-IKKα, shRNA-IKKβ, shRNA-IKKi, shRNA-p50, or shRNA-p65, respectively. Luciferase activity was measured 72 h post-transfection. *D,* effect of MG132 on the MAT II enzyme activity and *MAT2A* gene expression regulated by *HBx*. HepG2 cells were transfected with pcDNA-HBx and treated with MG132 at different concentrations as indicated. MAT II activity was measured (*top panel*), and *MAT2A* and *GAPDH* mRNA levels were determined by RT-PCR (*lower panel*) 72 h post-transfection. *E,* effect of shRNA to *CREB* on the MAT II enzyme activity and *MAT2A* gene expression regulated by HBx. HepG2 cells were co-transfected with pcDNA-HBx and pshRNA-CREB. MAT II activity was measured (*top panel*), and *MAT2A* and *GAPDH* mRNAs were determined RT-PCR (*lower panel*) 72 h post-transfection.

CREB. These results further demonstrated that the *NF-κB* and *CREB* signaling pathways play critical roles in HBx-mediated *MAT2A* expression in hepatoma cells.

HBx Inhibits Hepatoma Cell Apoptosis by Activating MAT2A and MAT2β Expression and Inhibiting MAT1A Expression and AdoMet Production—The molecular mechanisms underlying the roles of *HBx* in the inhibition of apoptosis in liver cancer cells are not clear. Considering the facts that *HBx* stimulates *MAT2A* expression in human HCC and that activation of *MAT2A* inhibits apoptosis of liver cancer cells by reducing hepatic AdoMet levels, we speculated that activation of *MAT2A* mediated by *HBx* may link to its anti-apoptotic effect on hepatoma cells due to altered AdoMet production.

To test this hypothesis, HepG2 cells were co-transfected with a plasmid expressing shRNA specific to *MAT2A* along with pcDNA-HBx or control plasmid. Changes in nuclear morphology of transfected cells were examined by staining nuclear DNA with DAPI. Results showed that a small proportion of cells with typical hallmarks of apoptosis, such as nuclear fragmentation and chromatin condensation, were detected in cells transfected with pcDNA-3.1 (Fig. 7*A, panel a*). The numbers of apoptotic cells were decreased in the presence of *MAT2A* (Fig. 7*A, panel b*) or *HBx* (Fig. 7*A, panel c*), respectively, indicating *MAT2A* and *HBx* had an inhibitory effect on apoptosis in hepatoma cells. In addition, the numbers of apoptotic cells were increased after treating with shRNA specific to *MAT2A* in the absence

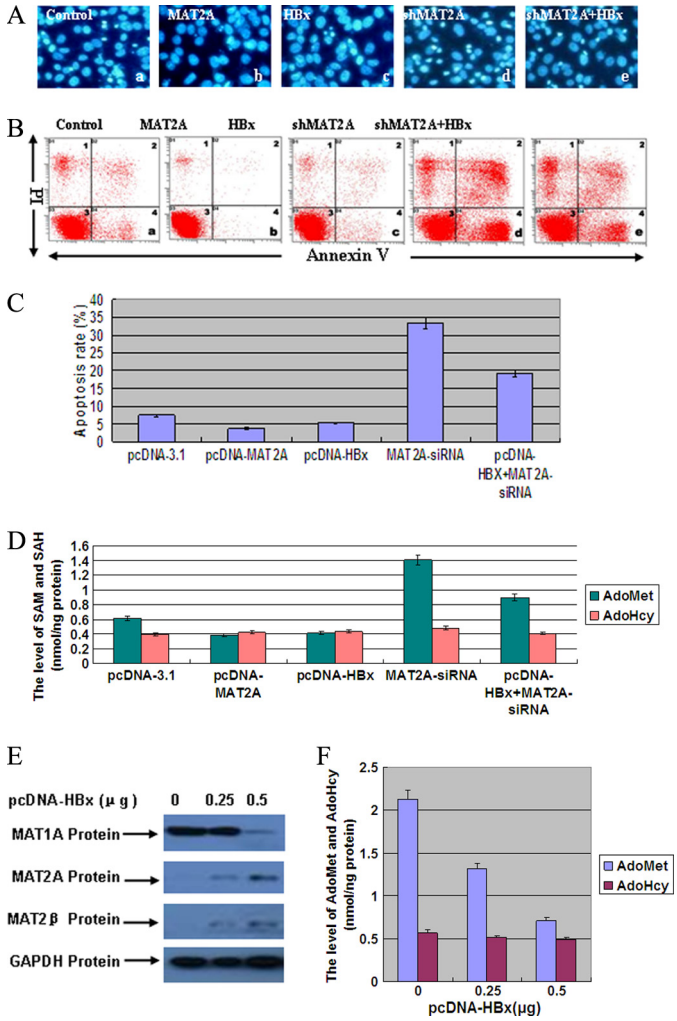

FIGURE 7. **Effects of *HBx* and *MAT2A* on cell apoptosis and AdoMet production in hepatoma cells.** HepG2 cells were plated at a density of 2×10^5 cells/cm^2. *A* and *B*, HepG2 cells were transfected with pcDNA-3.1 (*panel a*), pcDNA-MAT2A (*panel b*), pcDNA-HBx (*panel c*), pMAT2A-shRNA (*panel d*), and pcDNA-HBx plus pMAT2A-shRNA (*panel e*). *A*, changes in nuclear morphology of transfected cells were examined by staining of nuclear DNA with DAPI and visualized under fluorescence microscopy. *B*, rates of apoptosis were evaluated by the determination of sub-G_1 populations of transfected cells through Guava Nexin-V assays using flow cytometry. *C*, rates of apoptosis were summarized from flow cytometry analyses. *D*, levels of AdoMet and AdoHcy produced in transfected cells were determined by reverse phase-HPLC. Results in *C* and *D* are means of three independent experiments, and the *bars* represent ± S.D., significantly different from control by Turkey test. *E*, effects of HBx on the expression of *MAT* genes. L02 cells were transfected with pcDNA-HBx at different concentrations as indicated. The levels of MAT1A, MAT2A, MAT2β, and GAPDH proteins were determined using antibodies to the four proteins respectively. *F*, effects of HBx on the change in AdoMet homeostasis. L02 cells were transfected with pcDNA-HBx at different concentrations as indicated. The levels of AdoMet and AdoHcy were measured by HPLC. Results were mean of three independent experiments, significantly different from control by Turkey test.

(Fig. 7*A*, *panel d*) or presence of *HBx* (Fig. 7*A*, *panel e*), suggesting the anti-apoptotic effect on hepatoma cells was due to the expression of *MAT2A*.

The rates of apoptosis were further evaluated by flow cytometry analyses of sub-G_1 populations of apoptotic cells (Fig. 7, *B* and *C*). Results showed that the percentage of apoptotic cells was decreased from 13.07 ± 2.96% in the presence of pcDNA-3.1 (Fig. 7, *B, panel a,* and *C*) to 3.72 ± 0.69 and to 5.24 ± 0.85% in the presence of MAT2A (Fig. 7, *B, panel b,* and *C*) and HBx (Fig. 7, *B, panel c,* and *C*), respectively. However, the percentage of apoptotic cells was increased to 33.21 ± 6.65 and 19.31 ± 5.13% when MAT2A was knocked down by shRNA in the absence (Fig. 7, *B, panel d,* and *C*) and presence (Fig. 7, *B, panel e,* and *C*) of *HBx*, respectively ($p < 0.01$). These results again suggested that the anti-apoptotic effect on hepatoma cells was due to the expression of *MAT2A*.

TABLE 2
Changes in AdoMet, MTA, AdoHcy levels in HepG2 cells regulated by the different concentrations of HBx

HBx	AdoMet	MTA	AdoHcy	AdoMet/AdoHcy
μg				
0	0.72 ± 0.16	0.41 ± 0.08	0.35 ± 0.06	2.1 ± 0.05
0.25	0.51 ± 0.12[a]	0.38 ± 0.05	0.32 ± 0.03	1.6 ± 0.04[a]
0.50	0.37 ± 0.09[a]	0.36 ± 0.06	0.31 ± 0.04	1.0 ± 0.01[a]

[a] $p < 0.05$ *versus* HBx 0 μg by unpaired Student's *t* test. Results represent means ± S.E. from four to five separate determinations.

Because inhibition of apoptotic cell death in hepatoma cells by *MAT2A* may result from a reduction of AdoMet levels, we evaluated the changes in the concentrations of AdoMet under the conditions of knockdown of *MAT2A* and overexpression of *MAT2A* or *HBx* in transfected cells, respectively. Results showed that AdoMet levels were slightly reduced when *MAT2A* or *HBx* was present, as compared with the control, although they increased when the *MAT2A* gene was knocked down by shRNA in the absence or presence of HBx (Fig. 7*D*). However, AdoHcy levels remained relatively unchanged under the same conditions (Fig. 7*D*).

The preservation of MAT1A expression and MATI/III activity is a fundamental trait of the healthy and differentiated hepatocyte. Loss of *MAT1A* expression results in the malignant transformation of the liver, although the replacement of MATI/III by MATII appears to confer a growth advantage to the transformed cell. Thus, we further determined the effects of *HBx* on the expression of MAT proteins (*MAT1A, MAT2A,* and *MAT2β*) by Western blot analyses. Results showed that in the absence of *HBx, MAT1A* was highly expressed, and *MAT2A* or *MAT2β* was not detected, but in the presence of *HBx, MAT1A* expression was inhibited, and *MAT2A* or *MAT2β* expression was induced (Fig. 7*E*).

The effects of *HBx* on the production of AdoMet and AdoHcy were also determined. Results indicated that *HBx* inhibited AdoMet production in an HBx dose-dependent manner but did not affect AdoHcy production (Fig. 7*F*). In the effort to analyze the effects of HBx on the levels of AdoMet, MAT, and AdoHcy, we found that a 30% reduction in intracellular AdoMet production was detected in HepG2 cells transfected with 0.25 μg of pcDNA-HBx, and a further 50% reduction in AdoMet production was measured in cells transfected with 0.50 μg of pcDNA-HBx (Table 2). The ratio of AdoMet:AdoHcy was decreased in parallel with the AdoMet level, whereas AdoHcy and MTA level remained relatively unchanged (Table 2). These results demonstrated that *HBx* inhibits hepatoma cell apoptosis by activating *MAT2A* and *MAT2β* expression and inhibiting *MAT1A* expression and AdoMet production.

DISCUSSION

Hepatitis B virus is a major causative agent of acute and chronic hepatitis in humans and is closely associated with the incidence of human HCC (20). The X protein of HBV is essential for transactivation of the viral and some cellular genes (21, 22). Epidemiological and molecular evidence indicates that *HBx* is involved in the development of primary HCC (23, 24). *HBx* is reported to induce liver cancer growth in transgenic mice and to activate several host genes important for cell proliferation and transformation, such as c-*fos*, c-*myc*, and β-interferon. *HBx* is a trans-activating protein that alters gene expression by interacting with transcription factors or stimulating signaling pathways that promote cell growth and survival. *HBx* also binds to and inactivates tumor suppressors and senescence-related factors (25, 26). However, the mechanisms behind the role of *HBx* in the regulation of HCC development remain largely unknown.

In this study, we identified *MAT2A* as a new target of *HBx*. *HBx* activates the *MAT2A* promoter and induces its expression in hepatic cell line (L02) and hepatoma cell lines (HepG2 and BEL-7404) in a dose-dependent manner, indicating *HBx* is capable of regulating *MAT2A* expression. To gain insight into the mechanism behind the function of *HBx* in the regulation of *MAT2A* expression, a series of mutations of *MAT2A* promoter were constructed and assayed. Our results indicated that the sequence between nt −548 and −108 of the promoter of the *MAT2A* gene along with *NF-κB2* and *CREB* recognition elements are required for the function of *HBx* in the activation of *MAT2A* expression. *HBx* facilitates the binding of *NF-κB* and *CREB* to the *MAT2A* promoter. In addition, we further confirmed that *NF-κB* and *CREB* signal transduction pathways are involved in the activation of *MAT2A* expression regulated by *HBx* in hepatoma cells. These results suggested that one of the mechanisms in which HBx regulates HCC development is through activating *MAT2A* expression.

In mammals, two genes (*MAT1A* and *MAT2A*) encode two homologous catalytic subunits of the MAT enzyme. Normal liver expresses *MAT1A*, whereas *MAT2A* is induced in human HCC and facilitates cancer cell growth (27, 28). Studies have shown that a switch in gene expression from *MAT1A* to *MAT2A* in human liver cancer is pathogenetically important, as stimulation of *MAT2A* expression in cancer cells enhances cell growth through DNA hypomethylation, whereas inhibition of *MAT2A* expression in hepatoma cells has a reverse phenotype (29, 30). Thus, *MAT2A* functions as a positive regulator in hepatoma growth, suggesting that manipulating *MAT2A* expression may have therapeutic potential for the treatment of hepatoma.

MAT2A is transcriptionally induced in human HCC and in rodents during rapid liver growth and dedifferentiation. Many studies have shown that increased *MAT2A* expression provides liver cancer cells a growth advantage by inhibiting cellular apoptosis. HBx protein also can inhibit cell apoptosis during the development of HBV-associated HCC. The anti-apoptotic effect shared by *HBx* and *MAT2A* prompted us to examine the effects of *HBx* on *MAT2A* activation and cell apoptosis in hepatoma cells. Our results showed that both *HBx* and *MAT2A* inhibit cell apoptosis in HepG2 cells. In contrast, knockdown of *MAT2A* expression by shRNA induces cell apoptosis in hepatoma cell, even in the presence of *HBx*. These results suggested that *MAT2A* is a downstream target of *HBx* and may partially explain the anti-apoptotic effect of HBx on the development of HBV-associated HCC.

However, the roles of *HBx* and its regulatory effect on apoptosis are still controversial, with some studies showing pro-apoptotic effects (31–33). In fact, *HBx* is known to localize in both the mitochondria and the nuclei of cells and subsequently modulates mitochondrial membrane potential and transcription of certain genes, suggesting that the status and localization of *HBx* for the regulation of *NF-κB* activation and apoptosis may be changed according to the processing phase of its functional activity within a cell.

MAT enzyme activity is required for the production of AdoMet, because AdoMet is synthesized from methionine and ATP in a reaction catalyzed by the enzyme (34). In normal liver cells, two mechanisms to maintain the high cellular level of AdoMet are as follows: 1) up-regulation of *MAT1A* expression by AdoMet with the increase in MAT I/III activity, and 2) the high capacity of MAT I/III to convert dietary methionine and ATP into AdoMet. Because AdoMet down-regulates *MAT2A* expression and inhibits MAT II activity, the contribution of MAT II to the production of AdoMet is minimal in liver cells (15). AdoMet has rapidly moved from being a methyl donor to a key metabolite that regulates hepatocyte growth, death, and differentiation (35–38). In hepatocytes, AdoMet levels are related to the differentiation status of the cells. AdoMet levels are at high in quiescent and at low in proliferating hepatocytes during liver regeneration. The high level of hepatic AdoMet is transient. If the high level of hepatic AdoMet was persisting, it would favor a proliferative phenotype and ultimately the development of HCC (39, 40).

Liver injury caused by hepatotoxins or partial hepatectomy initiates a cellular response that involves a vast number of growth factors and cytokines (such as *HGF, TNF-α,* and *IL-6*) and generation of oxidative stress (*NO* and *ROS*), which leads to the inactivation of MAT I/III and a reduction of hepatic AdoMet level. This reduction in AdoMet level induces *MAT2A* expression and MAT II activity, which results in a new and lower steady state level of AdoMet. The reduced level of hepatic AdoMet releases the inhibitory effect of this molecule on the proliferative activity of hepatocyte growth factor, which facilitates liver regeneration. If the conditions leading to oxidative stress persist (*e.g.* chronic HBV infection), the hepatic levels of AdoMet are continuously low, which predisposes the liver to develop steatohepatitis, cirrhosis, and ultimately HCC (39, 40). In the cirrhotic liver, *MAT1A* expression is progressively silenced by a mechanism that involves the methylation of the gene promoter and its association with hypoacetylated histones (15).

In cancerous liver cells, MAT activity is very high when methionine is at low physiological concentrations (50 – 80 μM). However, in cultured normal rat and human hepatocytes, MAT activity is also very high when methionine concentrations are high (5 mM) (41). This led us to speculate that *MAT2β*, a regulatory subunit of *MAT2A*, is activated in response to HBx stim-

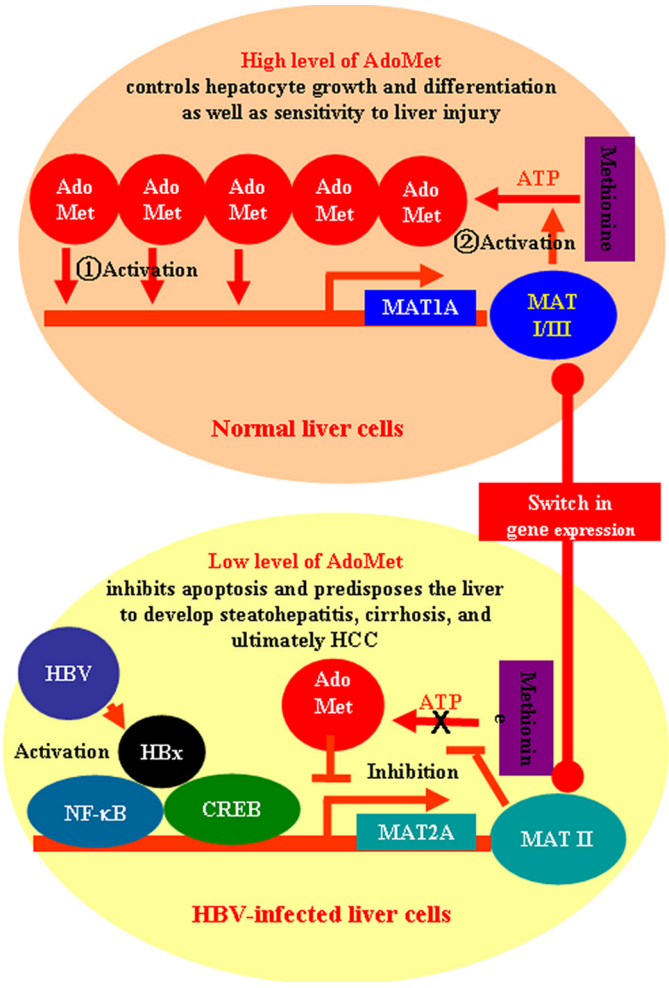

FIGURE 8. **Proposed model for the role of *HBx* in *MAT2A* expression, AdoMet production, cell apoptosis, and perhaps HCC development.** *Top,* in normal liver cells, two mechanisms to maintain the high cellular AdoMet level are as follows: ① up-regulation of *MAT1A* expression by AdoMet with the increase in MAT I/III activity; and ② the high capacity of MAT I/III to convert dietary methionine and ATP into AdoMet. Because AdoMet down-regulates *MAT2A* expression and inhibits MAT II activity, the contribution of MAT II to the production of AdoMet is minimal in liver cells. AdoMet controls liver growth and also regulates apoptosis with an anti-apoptotic effect on normal hepatocytes. *Bottom,* during HBV infection, the viral protein *HBx* activates *MAT2A* expression and MAT II activity by enhancing the binding of *NF-κB* and *CREB* to *MAT2A* gene promoter. *MAT2A* facilitates cancer cell growth through DNA hypomethylation, and thus, it functions as a positive regulator in hepatoma growth. In addition, in gene expression, highly expressed *MAT2A* inhibits *MAT1A* expression, which is progressively silenced by a mechanism that involves the methylation of the *MAT1A* gene promoter and its association with hypoacetylated histones. As a result, a new lower steady state level of AdoMet is reached. Such reduction in AdoMet level releases the inhibitory effect of this molecule on proliferation, which facilitates liver regeneration. If the conditions leading to chronic HBV infection are persistent, *MAT2A* levels are maintained continuously high, and AdoMet levels are maintained continuously low, which result in the inhibition of apoptotic cell death and predisposes the liver to develop steatohepatitis, cirrhosis, and ultimately HCC.

ulation. MATII can reduce the K_m value for methionine and the K_i value for AdoMet, making the subunit more susceptible to feedback inhibition (42). The steady state AdoMet level should be lower when the level of MAT2A is higher due to this feedback regulation. Our results showed that a sharp decrease of *MAT1A* protein levels and increases of MAT2A and MAT2β protein levels were detected in the presence of *HBx* in hepatocytes. In accordance with changes of the expression of *MAT* genes, the intracellular AdoMet levels were remarkably decreased in response to HBx stimulation.

AdoMet not only controls liver growth but also regulates apoptosis, with an anti-apoptotic role in normal hepatocytes and a pro-apoptotic role in liver cancer cells (43–45). *MAT2A* inhibits apoptosis of liver cancer cells, contributing to a reduction of steady state AdoMet levels. The reduction in hepatic AdoMet levels can feed into a vicious cycle that favors a switch in MAT expression and liver dedifferentiation (29). In an effort to investigate the effect of *MAT2A* on the changes in AdoMet levels and cell apoptosis regulated by HBx, we demonstrated that the changes in hepatoma cell apoptosis were concomitant with changes in AdoMet production. Knockdown of *MAT2A* expression by shRNA stimulated AdoMet production, and thus abolished the inhibitory effect of HBx on apoptosis in HepG2 cells. These results suggested that *MAT2A* and AdoMet act oppositely to the inhibition of apoptosis in hepatoma cells regulated by HBx.

In summary, we demonstrated that the X protein of HBV directly regulates the expression of *MAT2A* gene in hepatoma cells by enhancing the binding of transcription factors *NF-κB* and *CREB* to the promoter of the *MAT2A* gene. We proposed that during HBV infection, the viral protein HBx stimulates the expression of *MAT2A* gene, resulting in an increase of MAT II enzyme activity, a decrease of AdoMet production, and the inhibition of apoptotic cell death in cancer cells (Fig. 8). Our results suggested that HBx-induced *MAT2A* expression may play an important role in HBV-mediated HCC progression, which would provide new insights into our understanding the molecular mechanisms involved in the development of HCC caused by HBV infection.

Acknowledgment—We thank Dr. Yan Wang for input and assistance in the data analysis.

REFERENCES

1. Assrir, N., Soussan, P., Kremsdorf, D., and Rossignol, J. M. (2010) *Front. Biosci.* **15,** 12–24
2. Benhenda, S., Cougot, D., Buendia, M. A., and Neuveut, C. (2009) *Adv. Cancer Res.* **103,** 75–109
3. Feitelson, M. A., and Lee, J. (2007) *Cancer Lett.* **252,** 157–170
4. Chan, D. W., and Ng, I. O. (2006) *J. Pathol.* **208,** 372–380
5. Cheng, A. S., Wong, N., Tse, A. M., Chan, K. Y., Chan, K. K., Sung, J. J., and Chan, H. L. (2007) *Cancer Lett.* **253,** 43–52
6. Zhang, X., Zhang, H., and Ye, L. (2006) *J. Lab. Clin. Med.* **147,** 58–66
7. Moon, E. J., Jeong, C. H., Jeong, J. W., Kim, K. R., Yu, D. Y., Murakami, S., Kim, C. W., and Kim, K. W. (2004) *FASEB J.* **18,** 382–384
8. Robinson, W. S. (1994) *Annu. Rev. Med.* **45,** 297–323
9. Lee, A. T., and Lee, C. G. (2007) *Front. Biosci.* **12,** 234–245
10. Tang, H., Oishi, N., Kaneko, S., and Murakami, S. (2006) *Cancer Sci.* **97,** 977–983
11. Cougot, D., Wu, Y., Cairo, S., Caramel, J., Renard, C. A., Lévy, L., Buendia, M. A., and Neuveut, C. (2007) *J. Biol. Chem.* **282,** 4277–4287
12. Ye, L., Qi, J., Li, G., Tao, D., and Song, S. (2007) *J. Huazhong. Univ. Sci. Tech. Med. Sci.* **27,** 167–169
13. Clippinger, A. J., Gearhart, T. L., and Bouchard, M. J. (2009) *J. Virol.* **83,** 4718–4731
14. García-Trevijano, E. R., Latasa, M. U., Carretero, M. V., Berasain, C., Mato, J. M., and Avila, M. A. (2000) *FASEB J.* **14,** 2511–2518
15. Mato, J. M., Corrales, F. J., Lu, S. C., and Avila, M. A. (2002) *FASEB J.* **16,** 15–26

16. Wang, Q., Liu, Q. Y., Liu, Z. S., Qian, Q., Sun, Q., and Pan, D. Y. (2008) *J. Exp. Clin. Cancer Res.* **27,** 72–78
17. Liu, Q., Wu, K., Zhu, Y., He, Y., Wu, J., and Liu, Z. (2007) *Hepatol. Res.* **37,** 376–388
18. Martínez-Chantar, M. L., Latasa, M. U., Varela-Rey, M., Lu, S. C., García-Trevijano, E. R., Mato, J. M., and Avila, M. A. (2003) *J. Biol. Chem.* **278,** 19885–19890
19. Pañeda, C., Gorospe, I., Herrera, B., Nakamura, T., Fabregat, I., and Varela-Nieto, I. (2002) *Hepatology* **35,** 1381–1391
20. Park, N. H., and Chung, Y. H. (2007) *Korean J. Hepatol.* **13,** 320–340
21. Bouchard, M. J., Wang, L., and Schneider, R. J. (2006) *J. Virol.* **80,** 4406–4414
22. Lu, S. C., and Mato, J. M. (2005) *Alcohol* **35,** 227–234
23. Lu, S. C., Huang, Z. Z., Yang, H., Mato, J. M., Avila, M. A., and Tsukamoto, H. (2000) *Am. J. Physiol. Gastrointest. Liver Physiol.* **279,** G178–G185
24. Liu, X., Zhang, S., Lin, J., Zhang, S., Feitelson, M. A., Gao, H., and Zhu, M. (2008) *Biochem. Biophys. Res. Commun.* **373,** 643–647
25. Ye, L., Dong, N., Wang, Q., Xu, Z., Cai, N., Wang, H., and Zhang, X. (2008) *Intervirology* **51,** 50–58
26. Zhang, J. L., Zhao, W. G., Wu, K. L., Wang, K., Zhang, X., Gu, C. F., Li, Y., Zhu, Y., and Wu, J. G. (2005) *Arch. Virol.* **150,** 721–741
27. Corrales, F. J., Pérez-Mato, I., Sánchez Del Pino, M. M., Ruiz, F., Castro, C., García-Trevijano, E. R., Latasa, U., Martínez-Chantar, M. L., Martínez-Cruz, A., Avila, M. A., and Mato, J. M. (2002) *J. Nutr.* **132,** 2377S–2381S.
28. Lu, S. C., and Mato, J. M. (2008) *J. Gastroenterol. Hepatol.* **23,** S73–S77
29. Yang, H., Huang, Z. Z., Wang, J., and Lu, S. C. (2001) *FASEB J.* **15,** 1507–1516
30. Latasa, M.U., Boukaba, A., García-Trevijano, E. R., Torres, L., Rodríguez, J. L., Caballería, J., Lu, S. C., López-Rodas, G., Franco, L., Mato, J. M., and Avila, M. A. (2001) *FASEB J.* **15,** 1248–1250
31. Chami, M., Ferrari, D., Nicotera, P., Paterlini-Bréchot, P., and Rizzuto, R. (2003) *J. Biol. Chem.* **278,** 31745–31755
32. Wang, W. H., Grégori, G., Hullinger, R. L., and Andrisani, O. M. (2004) *Mol. Cell. Biol.* **24,** 10352–10365
33. Liang, X., Liu, Y., Zhang, Q., Gao, L., Han, L., Ma, C., Zhang, L., Chen, Y. H., and Sun, W. (2007) *J. Immunol.* **178,** 503–510
34. Catoni, G. L. (1953) *J. Biol. Chem.* **204,** 403–416
35. Bradford, M. M. (1976) *Anal. Biochem.* **72,** 248–254
36. Avila, M. A., Carretero, M. V., Rodriguez, E. N., and Mato, J. M. (1998) *Gastroenterology* **114,** 364–371
37. Ramani, K., Yang, H., Xia, M., Ara, A. I., Mato, J. M., and Lu, S. C. (2008) *Hepatology* **47,** 521–531
38. Yang, H., Ara, A. I., Magilnick, N., Xia, M., Ramani, K., Chen, H., Lee, T. D., Mato, J. M., and Lu, S. C. (2008) *Gastroenterology* **134,** 281–291
39. Chiang, P. K., Gordon, R. K., Tal, J., Zeng, G. C., Doctor, B. P., Pardhasaradhi, K., and McCann, P. P. (1996) *FASEB J.* **10,** 471–480
40. Yang, H., Magilnick, N., Noureddin, M., Mato, J. M., and Lu, S. C. (2007) *J. Cell. Physiol.* **210,** 766–773
41. Cai, J., Sun, W. M., Hwang, J. J., Stain, S. C., and Lu, S. C. (1996) *Hepatology* **24,** 1090–1097
42. Halim, A. B., LeGros, L., Geller, A., and Kotb, M. (1999) *J. Biol. Chem.* **274,** 29720–29725
43. Yang, H., Sadda, M. R., Yu, V., Zeng, Y., Lee, T. D., Ou, X., Chen, L., and Lu, S. C. (2003) *J. Biol. Chem.* **278,** 50887–50896
44. Roje, S. (2006) *Phytochemistry* **67,** 1686–1698
45. Loenen, W. A. (2006) *Biochem. Soc. Trans.* **34,** 330–333